VALIDATION OF TURBULENCE MODELS FOR SIMULATION OF AXIAL FLOW COMPRESSOR

Marcelo R. Simões, marcelosimoes@petrobras.com.br
Petrobras/CENPES/Basic Engineering

Bruno G. Montojos, bgm87@lasme.coppe.ufrj.br
Programa de Engenharia Nuclear, COPPE/UFRJ, Brazil

Newton R. Moura, newton.moura@petrobra.com.br
Petrobras/CENPES/Gas and Energy

Jian Su, sujian@lasme.coppe.ufrj.br
Programa de Engenharia Nuclear, COPPE/UFRJ, Brazil

Abstract. *The aim of this work is to show the use of different turbulence models applied to CFD simulation of turbulent flow inside a rotor of an axial flow compressor of which flow field has been obtained experimentally in laboratory test. Turbulence models that provide the simulation results in good agreement with experimental data may be used in the design of new axial flow compressors. The turbulence models that were chosen are $\kappa - \epsilon$, $\kappa - \omega$, and SST. The results that came closer to the experimental data were the SST results, which allows us to conclude that this model is the most appropriate for the simulation of an axial flow compressor rotor.*
Keywords: *turbomachinery; CFD; turbulence models; axial flow compressor; SST; eddy-viscosity*

1. Introduction

The axial compressors are usually found in two applications: medium and large size gas turbine air compressor, and air compressor in the fluid cat craker units (FCC) in the oil industry and even in air blower in the iron and steel industry. For their inventive characteristics, they operate with high volume flow and moderate compression ratios. Their purchase price is higher than a centrifugal compressor's. Nevertheless, they have more thermodynamic efficiency which results in an energetic operational cost considerably inferior, thus we do not have to wait long to have the invested capital back.

According to Denton e Dawes (1999), the computational fluid dynamics probably have the most important role in a turbomachinery project than in any other application in engineering. For many years the project of a turbine or a modern compressor would be unimaginable without the help of CFD, and its reliance on CFD has been increasing, because more and more flow numerical predictability becomes propitious. Simulations in CFD are conducted during the project phases in order to obtain a qualitative analysis of the aerothermodynamic project. However, Marini et al. (2002) brings out that the use of CFD is strongly affected by the numerical methodology applied and the computational resources, since both interact between themselves.

The report presented by Dunham (1998) shows a study in which several specialists performed a blind test with the Rotor 37. In this test, several turbulence models were going to be analyzed, as well as different quantities of elements in the grid generated in order to trace a relation among them. However, the authors did not have access to the experimental data for comparison. Also, other specialists performed similar works, for instance Yamada et al. (2003), Ito et al. (2008), Benini e Biollo (2007), Calvert e Ginder (1999), Denton (1997), among others, but focusing in variants of the original work: flow on the blade edge, changes in the blade geometry, among others. Bardina et al. (1997) performed a research to evaluate and validate four known turbulence models: Wilcox two-equation $\kappa - \omega$ model, Launder and Sharma two-equation $\kappa - \epsilon$ model, Menter two-equation $\kappa - \omega / \kappa - \epsilon$ SST model, and Spalart and Allmaras one-equation model.

This work presents the application of a computational fluid dynamics tool (CFD) in the evaluation of the turbulent flow inside a transonic axial compressor rotor named NASA 37. The major objective of this work was to provide accurate numerical solution for the proposed problem and to compare the numerical results with available experimental data in the literature. Three available turbulence models were tested and validated against experimental data. The turbulence models selected, all being two-equation type, are standard $\kappa - \epsilon$, $\kappa - \omega$, and SST. The steps and details for the simulation preparation are presented. The compressor rotor performance curves obtained for each turbulence model and numerical results were compared with experimental data.

2. Mathematical Modeling

For the mathematical model, it was considered three dimensional, transient, turbulent flow of a Newtonian fluid with constant thermophysical properties. The continuity equation is:

$$\nabla \bullet \mathbf{U} = 0 \tag{1}$$

where ρ is the specific mass, $\mathbf{U}$ is the velocity vector and t is the time. The Reynolds averaged Navier-Stokes (RANS) equations are given by:

$$\frac{\partial \rho \mathbf{U}}{\partial t} + \nabla \bullet (\rho \mathbf{U} \otimes \mathbf{U}) - \nabla \bullet (\mu_{eff} \nabla \mathbf{U}) = \nabla p' + \nabla \bullet (\mu_{eff} \nabla \mathbf{U})^T + \mathbf{B} \tag{2}$$

where $\mathbf{B}$ is the body force vector, that is null in this study, μ_{eff} is the effective viscosity and p' is the turbulent modified pressure.

The turbulent modified pressure is defined by:

$$p' = p + \frac{2}{3}\rho k \tag{3}$$

where p is pressure, k is the turbulence kinetic energy.

The effective viscosity is given by:

$$\mu_{eff} = \mu + \mu_t \tag{4}$$

where μ_t is the turbulent eddy viscosity and μ is the molecular viscosity of the fluid.

In this work, it was employed the SST turbulence model - *Shear Stress Transport* (Menter, 1997, Menter et al., 2003) which was indicated for calculation of skin friction and heat flow at solid surface. This model used the $k - \omega$ near the wall and uses the $k - \epsilon$ far from the wall, where each one gives the better results.

The transformed equations for the $k - \epsilon$ and the $k - \omega$ for SST turbulence model are:

$$\frac{\partial (\rho k)}{\partial t} + \nabla \bullet (\rho \mathbf{U} k) = \nabla \bullet \mu + \mu_t \sigma_k \nabla k + \widetilde{P}_k - \beta^* \rho \omega k \tag{5}$$

$$\frac{\partial \rho \omega}{\partial t} + \nabla \bullet \rho \mathbf{U} \omega = \nabla \bullet \mu + \mu_t \sigma_\omega \nabla \omega + 2(1 - F_1)\rho \sigma_{\omega 2}\frac{1}{\omega}\nabla k \bullet \nabla \omega + \frac{\alpha}{\nu_t}P_k - \beta \rho \omega^2 \tag{6}$$

where ω is the turbulence frequency and $\nu_t = \mu_t/\rho$. P_k is the shear production of turbulence and its limits are defined by:

$$P_k = \tau : \nabla \mathbf{U} \quad \to \quad \widetilde{P}_k = \min(P_k, 10\beta^* \rho k \omega) \tag{7}$$

where the Reynolds stress tensor is given by $\tau = 2\mu_t \mathbf{D} - \frac{2}{3}\rho k \delta$, where $\mathbf{D} = \frac{1}{2}\nabla \mathbf{U} + \nabla \mathbf{U}^T$.

All the model constants are obtained by combination of the corresponding constants of the $k - \epsilon$ and $k - \omega$ model using a blending function F_1 by $\alpha = \alpha_1 F_1 + \alpha_2 (1 - F_1)$, where α_1 e α_2 are constants of the models $k - \omega$ and $k - \epsilon$ respectively.

The constants for this model are: $\beta^* = 0,09$, $\alpha_1 = 5/9$, $\beta_1 = 3/40$, $\sigma_{kl} = 0,85$, $\sigma_{\omega l} = 0,5$, $\alpha_2 = 0,44$, $\beta_2 = 0,0828$, $\sigma_{k2} = 1$ e $\sigma_{\omega 2} = 0,856$.

The first blending function F_1 is defined by:

$$F_1 = \tanh\left\{\left\{\min\left[\max\left(\frac{\sqrt{k}}{\beta^* \omega y}, \frac{500\nu}{y^2 \omega}\right), \frac{4\rho \sigma_{\omega 2}k}{CD_{k\omega}y^2}\right]\right\}^4\right\} \tag{8}$$

where $CD_{k\omega}$ is

$$CD_{k\omega} = \max\left(2\rho \sigma_{\omega 2}\frac{1}{\omega}\nabla k \bullet \nabla \omega, 10^{-10}\right) \tag{9}$$

which y is the distance to the nearest wall.

F_1 is equal to zero away from the surface ($k - \epsilon$ model), and switches to one inside the boundary layer ($k - \omega$ model). The turbulent eddy viscosity is defined as:

$$\nu_t = \frac{a_1 k}{\max(\quad a_1 \omega, SF_2)} \tag{10}$$

where $a_1 = 0,31$, S is the invariant measure of strain rate given by $\sqrt{2\mathbf{D} : \mathbf{D}}$ and F_2 is a second blending function defined by:

$$F_2 = \tanh\left[\left[\max\left(\frac{2\sqrt{k}}{\beta^* \omega y}, \frac{500\nu}{y^2 \omega}\right)\right]^2\right] \tag{11}$$

This model requires the knowledge of the distance between the nodes and the nearest wall. So, it is obtained a better interaction between the $k - \omega$ and $k - \epsilon$. The wall scale equation is solved to get these wall distances:

$$\nabla^2 \phi = -1 \tag{12}$$

Table 1. Rotor 37 main parameters

Parameter	Value
Rotor inlet hub-to-tip diameter ratio	0.7
Inlet blade tip diamenter	0.5074 m
Rotor blade aspect ratio	1.19
Rotor tip relative inlet Mach number	1.48
Rotor hub relative inlet Mach number	1.13
Rotor tip speed	454 m/s
Rotor tip solidity	1.29
Blade airfoil sections	Multiple Circular Arc (MCA)
Number of rotor blades	36

where ϕ is the value of the wall scale. The wall distance can be calculated from the wall through:

$$WD = \sqrt{|\nabla\phi|^2 + 2\phi} - |\nabla\phi| \qquad (13)$$

The mathematical model was solved numerically by using the commercial CFD package *ANSYS CFX-11.0*. This program uses numerical method of finite volume as solution (Element Based Finite Volume Method - EBFVM), which allows the solution of problems by blending of unstructured grids. Then, it is possible to obtain a numerical solution of discretized momentum and mass balance equations.

3. Experimental Validation

The compressor used in this work is known as NASA rotor 37, and the decision to use it was due to the great number of experimental test data information available, and also for the convenience of the compressor geometry availability in the CFX program examples package. This rotor was designed by the NASA and initially tested as part of a research program involving a four-stage axial compressor. These stages had the intention to shroud one zone of project parameters typically from an aero-derived gas turbine compressor.

In Figs. 1, 2 and 3 it is possible to observe the details in the tested compressor geometry according to the report gave out by Dunham (1998). Figures 4 and 5 show the drawing of the analyzed blade and rotor domain.
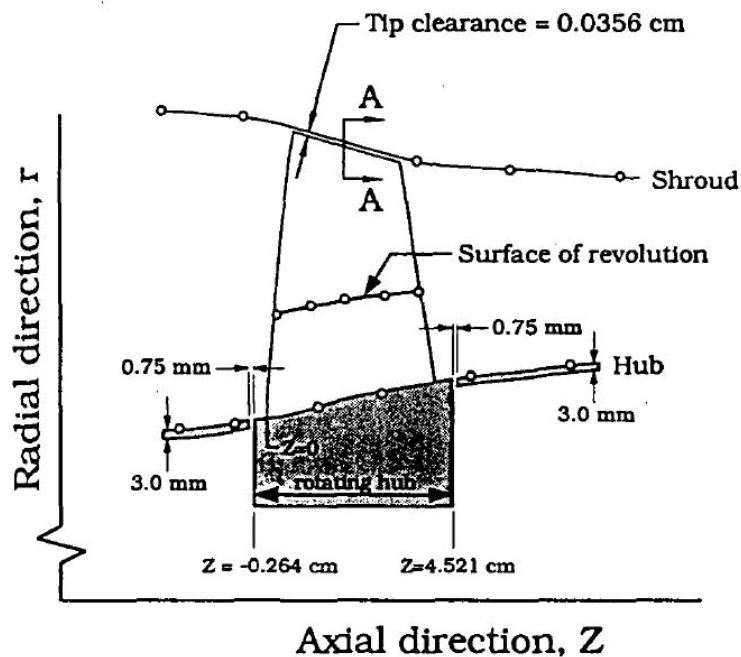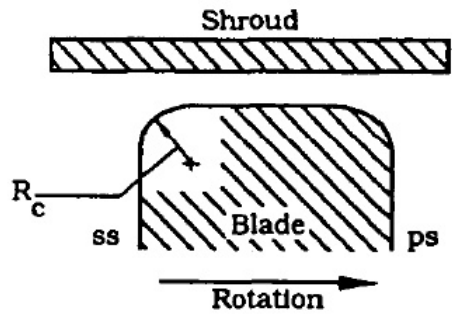

Figure 1. Rotor side view

View A-A

(Not to scale)

Note:
R_c = 0.0107 cm
Tip clearance = 0.0356 cm
at design speed

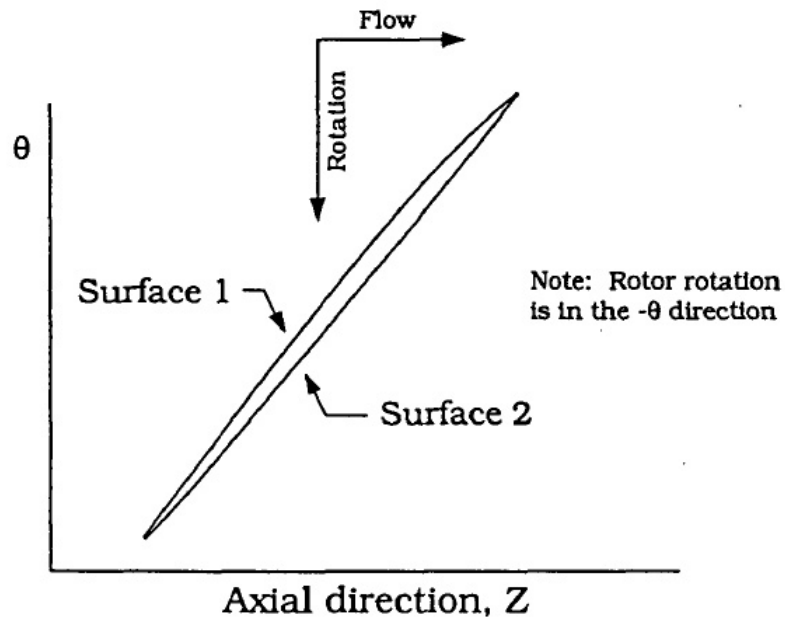Figure 2. Transversal view of a blade tip cut

Figure 3. Superior view of rotation direction and flow course

4. Computational Domain, Grid and Bondary Conditions

The simulation followed the experiment, the geometry dimension was the same with the exception that there was not extension until the inlet. The inlet fully developed turbulent channel flow was defined through an equation that was considered a good approximation for the case of the experimental Reynolds number.
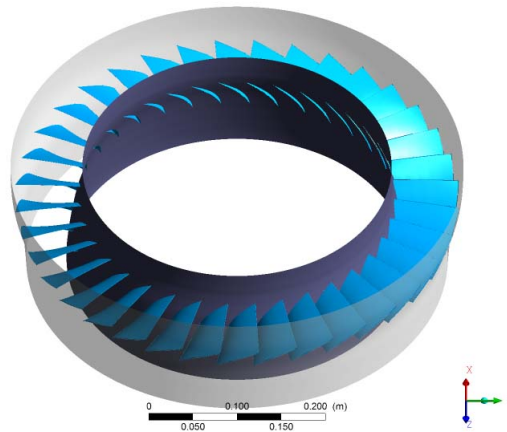
Figure 4. Rotor 37 in 3D
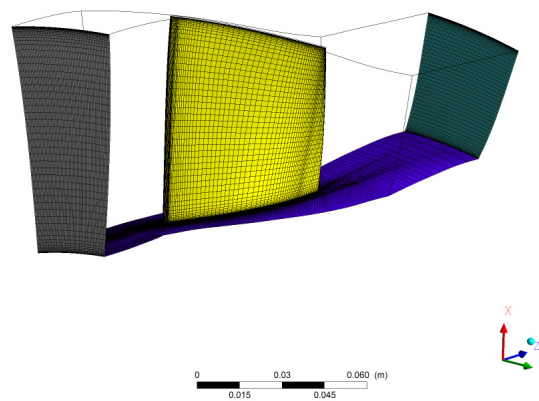
Figure 5. Control volume view

5. Results

The objective of this work was to analyze the response of three turbulence models, k-ϵ, k-ω and SST, available in a commercial CFD package using as the flow problem a transonic axial flow compressor rotor named NASA 37. Since the rotor is composed of 36 blades and the solution to the flow is periodic among them, we dealt only with one blade passage. It was not included in this work the guide vanes on the rotor input and the stator blades at the rotor outlet, not even their interaction with the rotor through the flow passage. The geometry, the grid and the boundary conditions used were the same, except for the flow in the outlet boundary and for the turbulence model used.

The performance curves were obtained, with 5 points for each rotor curve with each turbulence model. The main curves obtained were the ones of pressure ratio by normalized mass flow, and of adiabatic efficiency by normalized mass flow. The flow was normalized using as the maximum flow, or equal to 1, the compressor flow in choke equal to 20.93 kg/s. The program used in the computational simulations was the CFX, provided by ANSYS.

In Fig. 6 it is possible to observe that the SST turbulence model was the one closest to the real case curve of pressure ratio by normalized mass flow, in inclination as well as in accuracy. The results found by SST are better then the κ-ϵ model in the points close to the one of the machine project; nevertheless the κ-ϵ model was closer when the flow was nearby the

stall. The κ-ω model was the one which presented the worst results, overestimating the values of pressure ration in all the points of the curve. We can conclude from that graphic that the SST model overcame the others by reaching the closest results to the experimental data.

In Fig. 7 the three models present similar values for low flows. The adiabatic efficiency found by the SST model gets close to the experimental curve up to the normalized flow of 0.98, and shows more error to values above that limit. The curve performed by the κ-ϵ model remained parallel to the experimental adiabatic efficiency curve, getting closer in the values near the choke. Once more, the model κ-ω presented the worst results and did not reach the experimental data. We can conclude that both the κ-ϵ model and the SST found results close to the experimental curve with errors below 2.1%. It was not possible to find the rotor surge point with any of the turbulence models, because when it was tried the modeling of the compressor flow with 0.925 of normalized mass flow it was obtained results of reverse flow though the outlet face, what could be characterized as surge. The point of less flow evaluated was 0.93 of normalized mass flow.

In Figs. 8, 9 and 10 it is possible to observe the effect of chock waves in form of arch on the leading edge of the blade. The figures represent the mean Mach number contour for the height of 95% of the blade from the hub, with normalized mass flow of 0.98.
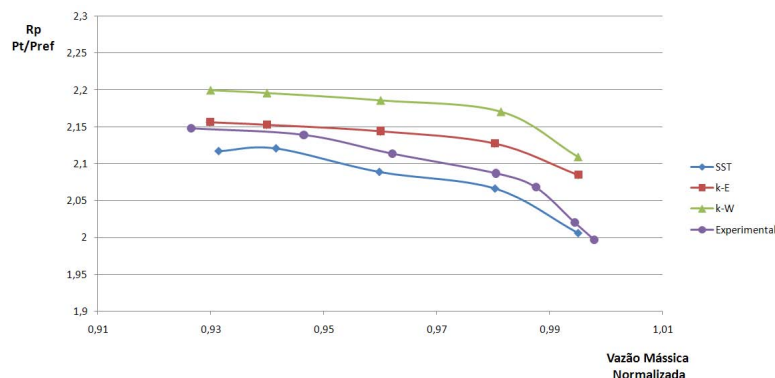

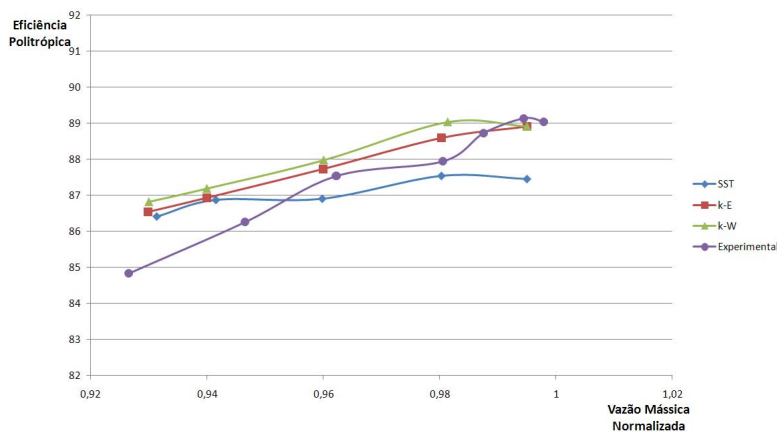Figure 6. Pressure ratio as a function of normalized mass flowrate

Figure 7. Adiabatic efficiency as a function of normalized mass flowrate

The figure 11 shows the graphic of temperature ratio by span%. From this graphic, we can easily conclude that the SST turbulence model overcame the others for having values much closer to the experimental ones. Again, the κ-ω model presented the worst results and the κ-ϵ model intermediary values.

The figure 12 shows the graphic of pressure ratio by span%. In this graphic it is possible to see that the values found by SST model remain close to the experimental values up to 60% of the span, and closer than the κ-ϵ model's for values above that limit. The κ-ω model once more presented slightly worse values. It is possible to conclude that the SST model reached the best accuracy when compared to the others.

The biggest absolute percentage errors estimated in the project point were found in the k-ω model around 5.4%, and in the SST and k-ϵ around 4.02%.
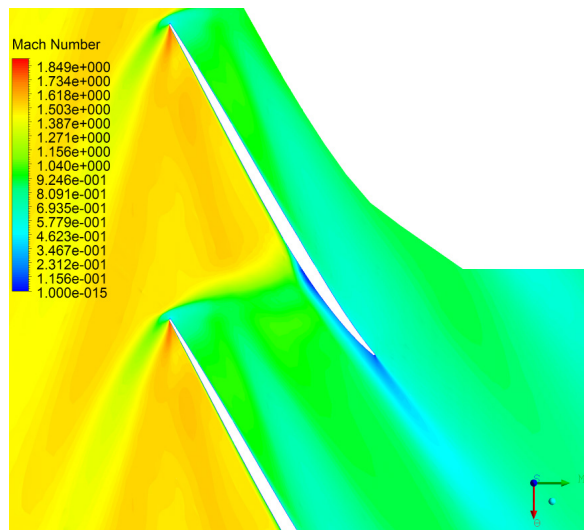
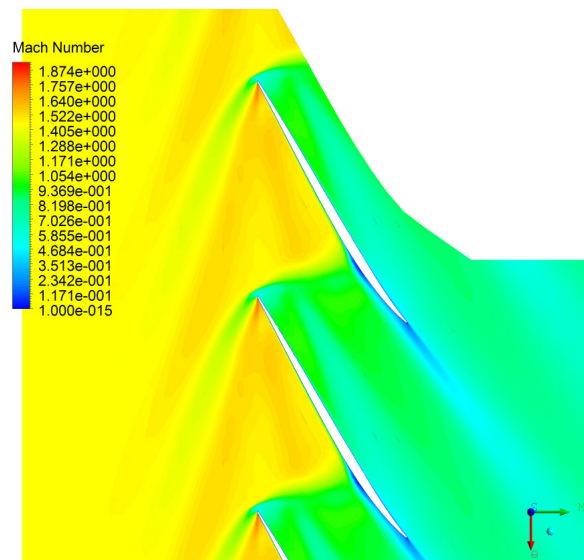Figure 8. k-ϵ, Mach number contour relating to 95% of span

Figure 9. k-ω, Mach number contour relating to 95% of span
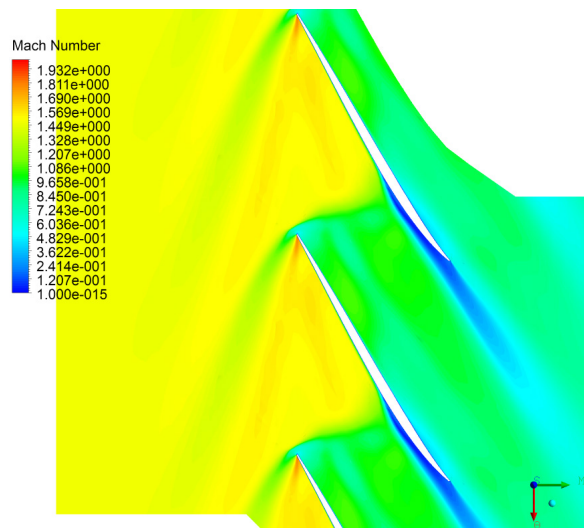

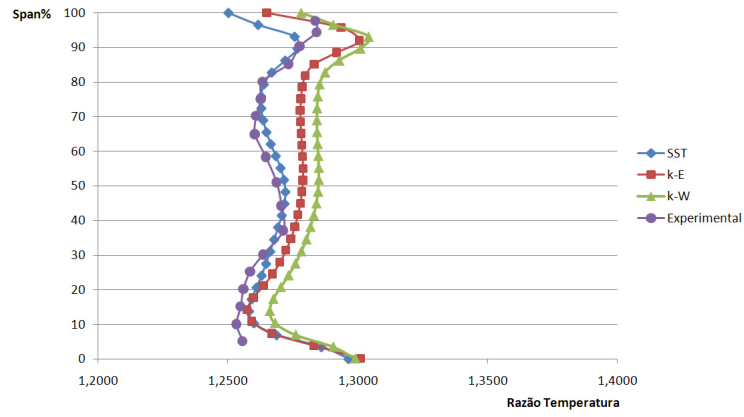Figure 10. SST, Mach number contour relating to 95% of span

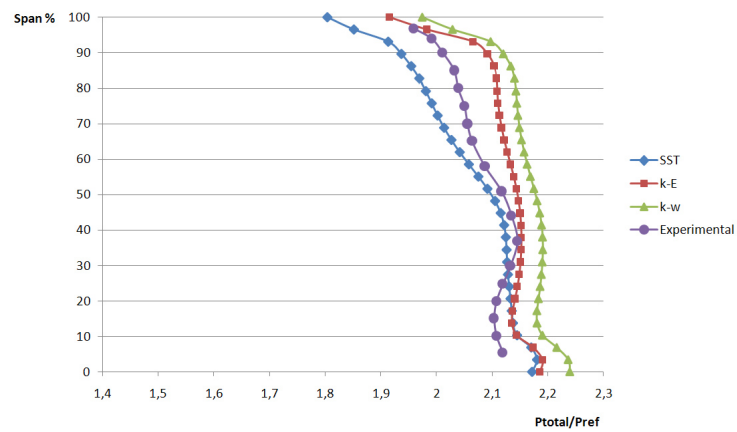Figure 11. Comparative graphic of temperature ratio by span

Figure 12. Comparative graphic of pressure ratio by span

6. Conclusions

The main objective of this work was to apply a computational fluid dynamics tool in the rotor performance evaluation of a transonic axial flow compressor named Rotor 37. Three turbulence models available in ANSYS CFX 11 were used: κ-ϵ, κ-ω and SST. Several simulations were performed under the same boundary conditions in order to make it possible the comparison among the models. The results found were used in the compressor performance curves survey to be compared with experimental data available in the literature. Finally, it was validated the model that best characterized the experimental test behavior.

It was concluded that the SST turbulence model was validated for this problem for presenting the most accurate results among the three models evaluated, when comparing them to the experimental data of the compressor performance. For this end, it was compared pressure ratio curves by normalized mass flow, adiabatic efficiency by normalized mass flowrate, total pressure ratio curves and temperature ratio in function of the rotor span%. As well, it was concluded that the turbulence model κ-ω did not achieve precise solutions for this flow type, and that the κ-ϵ model reached slightly worse results than the ones reported by SST.

7. Acknowledgements

8. References

Bardina, J. E., Huang, P. G., e Coakley, T. J. (1997). Turbulence modeling validation, testing, and development. Technical report, NASA TM 110446.

Benini, E. e Biollo, R. (2007). Aerodynamics of swept and leaned transonic compressor-rotors. *Applied Energy*, 84(10):1012–1027.

Calvert, W. J. e Ginder, R. B. (1999). Transonic fan and compressor design. *Proceedings of the Institution of Mechanical Engineers Part C-Journal of Mechanical Engineering Science*, 213(5):419–436.

Denton, J. D. (1997). Lessons from rotor 37. *Journal of Thermal Science*, 6(1):1–13.

Denton, J. D. e Dawes, W. N. (1999). Computational fluid dynamics for turbomachinery design. *Proceedings of the Institution of Mechanical Engineers Part C-Journal of Mechanical Engineering Science*, 213(2):107–124.

Dunham, J. (1998). Cfd validation for propulsion system components. Technical report, AGARD-AR-355.

Ito, Y., Watanabe, T., e Himeno, T. (2008). Effect of endwall contouring on flow instability of transonic compressor. *International Journal of Gas Turbine, Propulsion and Power Systems*, 2(1):24–29.

Marini, M., Paoli, R., Grasso, F., Periaux, J., e Desideri, J. A. (2002). Verification and validation in computational fluid dynamics: the flownet database experience. *Jsme International Journal Series B-Fluids and Thermal Engineering*, 45(1):15–22.

Menter, F. R. (1997). Eddy viscosity transport equations and their relation to the k-ϵ model. *Journal of Fluid Engineering*, 119(3):876–884.

Menter, F. R., Kuntz, M., e Langtry, R. (2003). Ten years of industrial experience with the sst turbulence model. in K. Hanjalic, Y. Nagano e M. Tummers (eds.), *Turbulence, Heat and Mass Transfer 4*, Begell House, Inc.

Yamada, K., Furukawa, M., Inoue, M., e Funazaki, K.-I. (2003). Numerical analysis of tip leakage flow field ina a transonic axial compressor rotor. In *Proceedings of the International Gas Turbine Congress*, Tokyo.

9. Responsibility notice

The authors are the only responsible for the printed material included in this paper